The influence of oxygen concentration on the formation of CuO and Cu$_2$O crystalline phases during the synthesis in the plasma of low pressure arc discharge

A.V. Uschakov[a,b], I.V. Karpov[a,b], A.A. Lepeshev[a,c] *, S.M. Zharkov[a,d]

[a] Siberian Federal University, 660041, Russia
[b] Reshetnev Siberian State Aerospace University, Krasnoyarsk, 660037, Russia
[c] Krasnoyarsk Scientific Center of the Siberian Branch of the Russian Academy of Science, 660036, Krasnoyarsk, Russia
[d] Kirensky Institute of Physics, Russian Academy of Sciences, 660036, Russia
* Corresponding author.
E-mail adress: sfu-unesco@mail.ru (A.A. Lepeshev)

Abstract. This paper describes the synthesis of copper oxide nanoparticles with different percentages of CuO and Cu$_2$O phases. It was achieved by the control of the percentage of oxygen in the gas mixture (N$_2$ + O$_2$) in a plasma-chemical process of evaporation-condensation by means of low-pressure arc discharge. In all the experiments, the pressure in the plasma-chemical reactor remained constant at 60 Pa. By means of X-ray diffraction (XRD), high resolution transmission electron microscopy (HRTEM), energy-dispersive X-ray spectroscopy (EDS), Fourier transform infrared spectroscopy (FTIR) it was found that the average particle size was 6 nm, and Cu$_2$O phase content decreases with increasing oxygen content in the gas mixture. High photocatalytic properties of Cu$_2$O powder were shown by the example of the reaction of the methyl orange dye decomposition in water solution. The problems, associated with the performance of this method and the formation of crystalline phases, are discussed.

Keywords: oxides; vapor deposition; X-ray diffraction; transmission electron microscopy (TEM); catalytic properties.

1. Introduction

Today production of devices and products, which apply the photocatalysis principle, is sustainably developed. For example, photocatalytic domestic and industrial air purifiers, antibacterial filters, steam-resistant glass and self-cleaning coatings for developing the exterior of city buildings and road infrastructure are now widely used. [1,2]

At the present moment the most widely-studied photoactive material is titanium dioxide. However, people continue searching for new materials that could compete with TiO$_2$. One of these materials can be the univalent copper oxide.

Copper oxide (I) – Cu$_2$O is a semiconductor of *p*-type with the bandgap width of 2.0-2.2 eV. In recent years, Cu$_2$O is studied intensively for the conversion of solar energy into electrical energy. Theoretically, the efficiency of this process for Cu$_2$O is 9-11%. Cu$_2$O is a promising material for the creation of Bose cells with high exciton binding energy (~150 meV). In addition, Cu$_2$O is a photocatalyst, working under the influence of visible light. [3] By means of the synthesis of particles with different size, it is possible to control the bandgap of Cu$_2$O while producing the photocatalysts with sensitivity to different wavelengths of visible light. Copper oxide, as a photocatalyst, can be used for the decomposition of water and for the organic contamination control. Cu$_2$O is also a promising magnetic semiconductor. [4]

The chemical methods allow supporting mass-production of nanopowders [5], but their structure is mainly amorphous. It is shown that the content of the amorphous structure reduces

photocatalytic reactivity and, consequently, the synthesis of nanocrystalline Cu_2O is of current importance. [6] The results of the chemical synthesis show that the time of calcination and the temperature strongly influence the nanopowder. [5] Thus, the problem of crystalline phase control during the growth of crystals from the nanoparticles, within large-scale production, remains difficult for any chemical method. Nanocrystalline particles with an average size of < 10 nm show higher photocatalytic properties than particles of larger size. [6] Thus, detailed investigation of Cu_2O nanoparticles is a significant research focus as well. It was shown that the thermal processes in plasma provide very efficient means for producing nanocrystalline materials taking into account their high temperature, high enthalpy and high speed of quenching, which causes the homogeneous condensation of the gas phase. [7,8]

Thus, considering the growing large-scale need in Cu_2O nanopowder, we used the method of condensation from the gas phase for the synthesis of Cu_2O with a proper crystalline phase. It is shown that the phase content of CuO and Cu_2O in the synthesized nanopowder can be controlled by choosing a suitable concentration of oxygen inside the chamber.

2. Experimental

The morphological structure of the samples was studied by using a JEOL JEM-2100 transmission electron microscope. The samples for electron microscopy investigations were prepared as follows: the powder was placed in isopropyl alcohol and was dispersed for 2 min in an ultrasonic bath, and then a drop of this solution was dripped on a carbon support film located on a TEM grid. The thickness of the carbon support film was 10-15 nm. The phase composition of the produced samples was studied by using Advance D8 X-ray diffractometer under the influence of CuK_α monochromatic radiation. Scanning was fulfilled at room temperature in the range of angles within 30–120° by 2θ with the interval of 0.04 deg. The specific surface area was measured by BJH method.

Spectral measurements of discharge plasma were carried out using a flexible optical fiber with a diameter of 0.5 mm, installed near the cathode of the evaporator. The applied part of the optical fiber was placed in the metal collimator with a diameter of 1.5 mm, which was exposed by applying negative potential (−300V) relative to the vacuum chamber, which allowed isolating the optical fiber from contact with the plasma and from dusting caused by the material of the cathode. The rest of the optical fiber was covered with an opaque plastic tube. The radiation of the plasma arc discharge was recorded by Ocean Optics HR4000 spectrometer. This spectrometer allows to record radiation spectra in the range of 200-1100 nm with a resolution of 0.7 nm.

The photocatalytic properties of Cu_2O were studied by the example of the reaction of photocatalytic decomposition of the dye (methyl orange) in water solution. The mercury-quartz lamp (arc tube mercury lamp) was used as a source of ultraviolet radiation. The preliminary washed Cu_2O powder (0.1 g), 200 ml of distilled water and 20 ml of 0.1 M solution of the dye was placed in the cell made from PMMA. Mixing was carried out in the cell with a mechanical stirrer. The hydrogen peroxide was used as an oxidizing agent in the reaction of decomposition, while the concentration of the agent at the beginning of the reaction was 1 mol/l. During the experiment, the samples were selected from the cell and centrifuged at the equal intervals of time (15 min). The change in dye concentration in the centrate was controlled through

spectrophotomer by changing the intensity of the dye absorption peak. The spectrophotometric measurements were performed by spectrophotometer SHIMADZU UV-3600 (206-23000).

The analysis of IR spectra was carried out by Nicolet 6700 IR Fourier spectrometer with a resolution of up to 0.09 sm^{-1} in the spectral range of 25000-20 sm^{-1}. The samples in the shape of granules were produced by using 100 mg of dry KBr and 2 mg of nanopowder.

The experimental equipment and the dependence of the powder properties on the spraying conditions are discussed. [9-12] The cathode consists of copper alloy M1 with diameter of 80 mm and length of 100 mm; it was placed on a water-cooled copper current lead. An auxiliary electrode was used to start the pilot arc, as it provided the plasma stream stabilization. The dimensions of the reaction chamber are 0.6 m in diameter and 0.6 m in height, with double walls and flanges made from stainless steel. The camera has two ports, one for viewing the arc column during evaporation of the metal, and the other for measuring the optical emission spectra (OES).

Plasma-generating nitrogen gas was fed through the evaporator and created a pressure of 60 Pa in the chamber. The capacity of the evaporator was 10 kW, the direct current of arc discharge was 100 A, the reaction gas was oxygen with the flow rate maintained at the level of 10, 20, 30 and 40 vol. % from the nitrogen supply. The oxygen was fed into the reactor in order to form a uniform shell around the plasma torch. The gas in reactor was preliminary evacuated up to the basic pressure of 10^{-3} Pa. The products of the reaction were collected during 10 min onto a hemispherical collector made from stainless steel with a water-cooling system, located at a distance of 0.12 m from the cathode. Below described the operating parameters of the reactor during the synthesis process.

- Base pressure in the chamber – 10^{-3} Pa;
- Arc discharge current – 100 A;
- Voltage – 70 V;
- Power – 10 kW;
- The cooling water supply through:

a) cathode – 1 l/min;
b) substrate – 1 l/min;
c) chamber wall – 2 l/min;

- Supply of plasma gas (nitrogen) – 60 Pa;
- Supply of reaction gas (oxygen) – 10, 20, 30 and 40 vol. % of O_2.

4. Results and Discussions

The rate of CuO synthesis at different oxygen concentrations was measured. The performance of vacuum plasma-chemical reactor was determined by measuring the loss in mass of the cathode material, and then using the measurements of the weight of the selected nanoparticles, synthesized at different oxygen concentrations. For concentrations of 10, 20, 30 and 40 vol.% of O_2, the resulted values were 35; 34.3; 22.1 and 21 g/h respectively. The loss of performance is caused by the intensification of the oxidation processes on the cathode surface. The efficiency of deposition of the material on the substrate was about 20% of the total nanoparticles weight. The bulk of the synthesized nanoparticles were deposited on the reactor walls. The nanoparticles, gathered on the substrate, were used for the further study.

Figure 1 shows X-ray diffraction spectra of the nanoparticles synthesized at different oxygen concentrations for values of 2θ in the range from 28° to 65°. The diffraction spectra of the

nanoparticles, synthesized at oxygen concentrations of 10 and 20 vol.% of O_2 from the nitrogen supply, clearly show the reflections (PDF 4+ #00-005-0667) corresponding cuprite structure of Cu_2O, *Pn3m* space group, other crystal structures were not found. Increasing the oxygen concentration up to 20 vol.% causes decreasing the crystallinity of the nanoparticles, therefore the grid parameter increases from 4.285 Å to 4.290 Å, which is significantly higher than the ones in the coarse-grained samples. Increasing the proportion of X-ray amorphous phase while increasing the concentration of oxygen is defined by the characteristic of plasma-chemical synthesis, when the oxygen saturation of the resulting nanoparticles occurs under a thermodynamically non-equilibrium conditions, with the violation of stoichiometry, as well as high residual stresses and defects of crystal structure. The diffraction spectrum of the nanoparticles synthesized at oxygen concentration of 30 vol.% of O_2 from the nitrogen supply shows that the reflections, corresponding to the monoclinic structure of CuO (PDF 4+ #00-045-0937) with lattice parameters a = 4.691 Å, b = 3.432 Å, c = 5.138 Å, appear in addition to the reflections corresponding to cuprite structure of Cu_2O. The reflections at 2θ = 35.915°, 44.189°, 58.396°, 64.210°, corresponding, evidently, to the transition tetragonal-distorted cubic crystal lattice of CuO, belonging to the space group $I4_1/amd$, are also presented. The proportion of CuO and Cu_2O, calculated according to the most intense lines of the diffraction spectrum, make up 65%. Further increasing the concentration of oxygen up to 40 vol.% of O_2 from the nitrogen supply, leads to a monotonic increase in the proportion of CuO up to 86%, according to the diffraction spectrum.
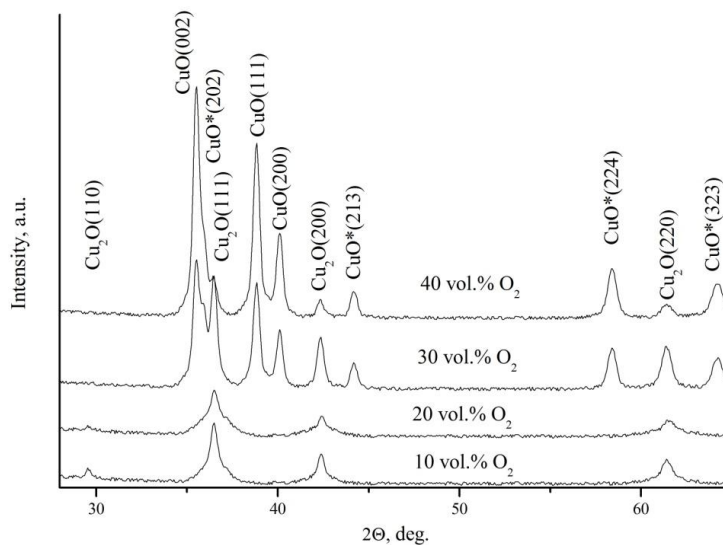

FIG. 1. X-ray diffraction spectra of the nanoparticles synthesized at different oxygen concentrations.

The sustainable growth of the monoclinic phase of copper oxide from 0 up to 86% means that the concentration of O_2 in the synthesis process deeply influences on the formation of crystalline phases. Fig. 1 also shows that high concentration of O_2 facilitates the formation of the monoclinic phase, while reducing the concentration of O_2 promotes the growth of cuprite phase of copper oxide.

Figure 2a shows a typical high-resolution transmission electron microscopy (HRTEM) image of the sample. The powder represents an ensemble of strongly agglomerated particles with irregular shape ranging from 4 to 9 nm in size. The particles up to 15 nm in size are also formed,

but they are, evidently, the agglomerates of smaller particles. These agglomerates cannot be disaggregated. These particles have a shape generally close to spherical one. The study of the granulometric composition shown that the NP has a lognormal distribution and the average particle size of 6 nm. The standard deviation was 1.2. The interpretation of the selected area electron diffraction (SAED) pattern (Fig. 2b) obtained from a group of the particles gives CuO phase with monoclinic structure (JCPDS data, No. 45-0937). This corresponds with the results obtained by the XRD spectrum.

The elemental composition of CuO nanopowder, with the ratio of gas mixture of 30% O_2 + 70% N_2, is given below (the content of the elements are given in at.%):

Cu – 52,70; O – 47,06; Si – 0,02; Cr – 0,02; Fe – 0,16; Ni – 0,02; Zn – 0,02. The elemental composition was determined using the Thermo Scientific ARL QUANT'X energy-dispersive X-ray fluorescence spectrometer.
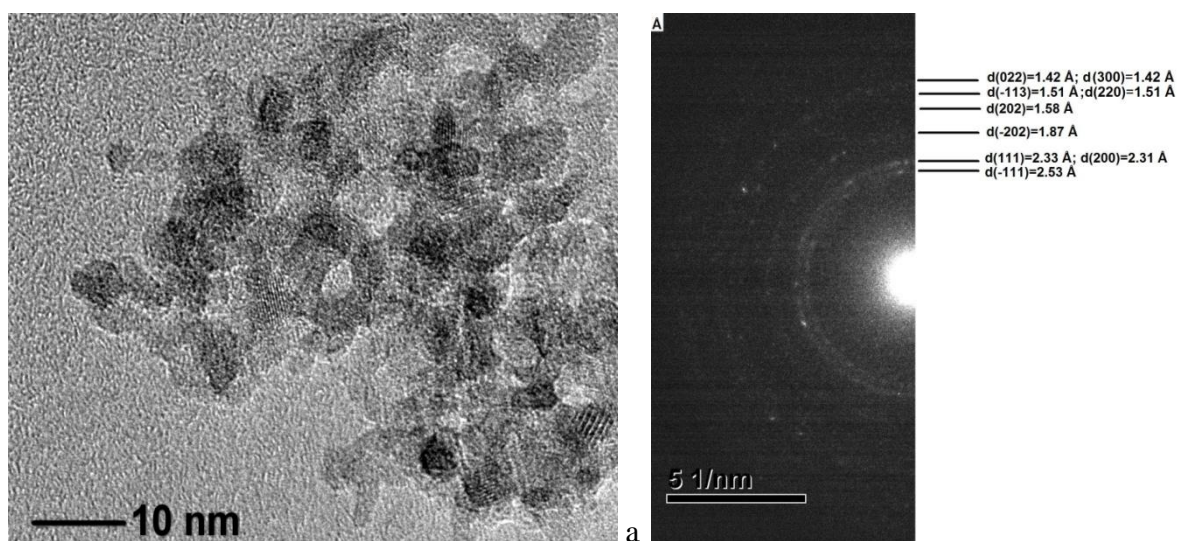

FIG. 2. HRTEM image (a) and SAED pattern (b) of the produced sample of copper oxide. The condition of synthesis: the pressure of N in the plasma-chemical reactor is 60 Pa, the concentration of O_2 is 30 vol.%.

Figure 3 presents the results of studying the optical spectra of radiation in the process of copper oxide synthesis in oxygen-containing plasma of low pressure arc discharge for different concentrations of oxygen, covering the spectral range between 200-1200 nm.
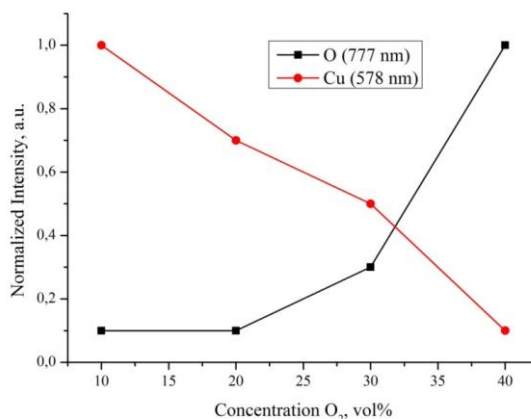
FIG. 3. Optical emission spectra in the process of copper oxide synthesis in oxygen-containing plasma of low pressure arc discharge for different concentrations of oxygen.

The main characteristics of the spectra correspond to the emission of excited ions of Cu (578.213 nm) and O (777.194 nm) produced directly in the process of impact ionization by the electron. [3] The results were normalized at its maximum peak. As the graphs show, the intensity of the emission lines of Cu is higher than those of O at low oxygen concentrations corresponding to the synthesis of Cu_2O. However, when the concentration of O increases, the intensity of the emission lines of O begins to dominate, it corresponds to the preferential synthesis of monoclinic CuO phase. The decrease in the intensity of emission lines of Cu with the increase of oxygen consumption is caused by two effects. First, increasing the concentration of oxygen intensifies chemical processes of oxidation on the cathode surface, which causes a decrease in the rate of cathode evaporation, as evidenced by a decrease in the output of the nanosized powder. Secondly, the intensity of plasma-chemical reactions is sharply increased and, consequently, causes more intense saturation by oxygen of copper clusters generated by arc evaporation. [13] It should be noted that the intensity of the emission lines of O increases sharply when the oxygen concentration is above 20 vol.%.

The value of the specific surface of the produced copper oxide nanopowder, calculated by the isotherm of low-temperature nitrogen adsorption, has amounted to 386 m^2/g. Applying the known ratio between the surface area S, pycnometric specific gravity $\rho = 6.3$ g/sm^3 and an average particle size of $d = 6/\rho S$, we get the result of 2.5 nm, which, however, does not comply with the data obtained by TEM. This noncompliance is explained by the fact that the condensate, dropped off on the surface of the particles, is much smaller than the basic powder. This condensate forms a rather porous "fur coat" around the particles and mainly determines the sorption activity of the powder. [14,15]

The FT-IR spectra of the nanoparticles synthesized at oxygen concentrations above 10 and 40 vol.%, is presented in Figure 4.
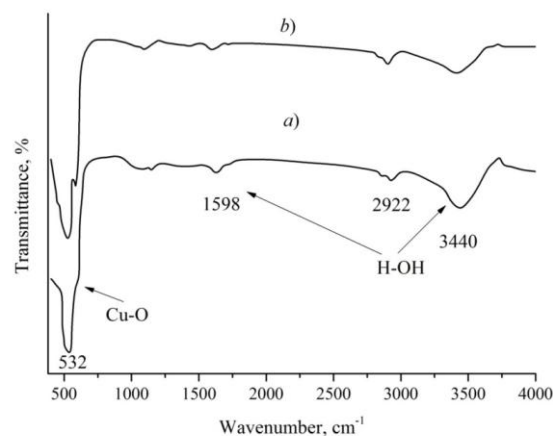

FIG. 4. The FT-IR spectra of the nanoparticles synthesized at oxygen concentrations above 10 (a) and 40 (b) vol.%.

The absorption frequencies of metal oxides are located usually in the area below 1000 sm^{-1} and arise from interatomic vibrations. As it can be seen from Figure 4a, the characteristic

symmetric and asymmetric frequencies for Cu_2O are observed at 1162 and 532 sm^{-1}, which corresponds to Cu(I)-O vibrations. [16,17] The CuO nanoparticles have similar characteristic frequencies (Figure 4b) at 1115 sm^{-1}. However, the appearance of two bands at 593 and 527 sm^{-1} can be attributed to Cu(II)-O vibrations, corresponding to the monoclinic CuO phase. [18] The similarity of the IR spectra of the nanoparticles produced in the plasma-chemical reactor at various concentrations of oxygen is defined by small particle sizes and the presence of several phases in the synthesized nanopowder, that was confirmed by XRD spectra.

The broad absorption band near 3414 sm^{-1} is observed in the near infrared spectra. It refers to the stretching vibrations of bound OH groups. [19] The presence of such groups is indirect evidence of high surface activity of the produced nanoparticles, appeared at high specific surface. In this case, a large number of available bonds formed on the surface of the particles, and the exposed atoms, such as Cu and O in the nanoparticles, could adsorb OH$^-$ and H$^+$ ions from their surrounding with a high probability, which could result in forming the surface enriched with active OH groups. The absorption band at 1622-1383 sm^{-1}, related to the deformation vibrations of water residue δ(HOH), is appeared in the spectrum of Cu_2O and CuO nanoparticles along with stretching vibrations of the bond OH groups.

To evaluate the photocatalytic activity of the produced Cu_2O nanoparticles, the reaction of photocatalytic decomposition of the methyl orange dye (MO) in water solution was used. The optical behavior of MO in the solution was analyzed by measuring its absorption spectra at 464 nm. The preliminary testing shows that without photocatalyst any degradation of the dye in solution does not observe. TiO_2 powder cannot be used for decomposition of MO in the visible range due to the large width of the forbidden zone (3.2 eV). Thus, in this case Cu_2O can be an effective catalyst. Figure 5 shows the absorption spectra of MO during its oxidation in the presence of nanosized Cu_2O powder synthesized at concentrations of 10 vol.% of O_2 and hydrogen peroxide under the influence of ultraviolet radiation.
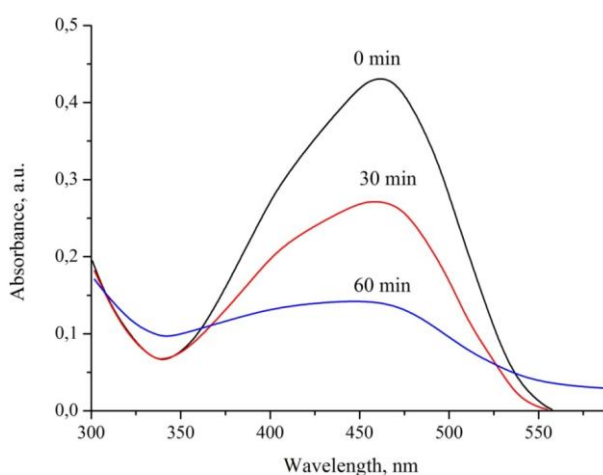

FIG. 5. The temporal evolution of the absorption spectra of MO with the addition of Cu_2O nanoparticles synthesized at oxygen concentration of 10 vol.%.

As the absorption spectra shows, the almost complete oxidation of the dye occurs after 60 min of irradiation process. The time of complete decolorization of methyl orange solution in the presence of nanosized copper oxide powder was 12 h. Comparing the catalytic activity of nanosized powder, obtained at different oxygen concentrations in plasma-chemical reactor, it

was found that the decay rate of MO is significantly higher in the presence of Cu_2O powder synthesized with 10 vol.% of O_2, that is caused, in our opinion, by low catalytic reactivity of CuO.

Thus, the effect of decomposition of poorly efflorescent dyes (for example, methyl orange) under the influence of Cu_2O nanoparticles was confirmed in our experiments.

5. Conclusion

The effect of oxygen concentration in the gas mixture of plasma-chemical reactor on the ratio of crystal phases of copper oxide nanoparticles has been investigated in this paper. Low concentration of O_2 facilitates the formation of cubic phase of Cu_2O, while the increase in O_2 concentration facilitates the growth of the monoclinic phase of CuO. The change in the crystalline phase, counting on the change of O_2 in the reactor, is associated with the caused by the cluster chemistry of vapor phase of condensation. Increasing the concentration of oxygen intensifies chemical processes of oxidation at the surface of the cathode, that causes a decrease in the rate of the cathode evaporation, the intensity of plasma-chemical reactions is sharply increases and, consequently, it leads to more intense oxygen saturation of copper clusters generated by arc evaporation.

The decomposition rate of MO is significantly higher with applying Cu_2O powder synthesized with 10 vol.% of O_2, that is caused, in our opinion, by low catalytic reactivity of CuO.

References

[1] Amy L Linsebigler, Guangquan. Lu, John T Yates (1995) Photocatalysis on TiO2 Surfaces: Principles, Mechanisms, and Selected Results, Chem Rev. doi:10.1021/cr00035a013.

[2] Ashkarran AA, Kavianipour M, Aghigh SM, Ahmadi Afshar SA, Saviz S, Iraji Zad A (2010) On the Formation of TiO_2 Nanoparticles Via Submerged Arc Discharge Technique: Synthesis, Characterization and Photocatalytic Properties, J Clust Sci. doi:10.1007/s10876-010-0333-7.

[3] Huang L, Peng F, Yu H, Wang H (2009) Preparation of cuprous oxides with different sizes and their behaviors of adsorption, visible-light driven photocatalysis and photocorrosion, Solid State Sciences. doi:10.1016/j.solidstatesciences.2008.04.013.

[4] Yang H, Ouyang J, Tang A, Xiao Y, Li X, Dong X, Yu Y (2006) Electrochemical synthesis and photocatalytic property of cuprous oxide nanoparticles, Research Bulletin. doi:10.1016/j.materresbull.2006.01.004.

[5] Li B, Wang X, Yan M, Li L (2002) Preparation and characterization of nano-TiO_2 powder, Mater Chem Phys. doi:10.1016/S0254-0584(02)00226-2.

[6] Gao L, Zhang Q (2001) Effects of amorphous contents and particle size on the photocatalytic properties of TiO_2 nanoparticles, Scr Mater. doi:10.1016/S1359-6462(01)00681-9.

[7] Fedorov LYu, Karpov IV, Ushakov AV, Lepeshev AA (2015) Influence of Pressure and Hydrocarbons on Carbide Formation in the Plasma Synthesis of TiC Nanoparticles, Inorganic Materials. doi:10.1134/S0020168515010057.

[8] Smolanov NA, Pankin NA (2014) On the structure and properties of a material deposited from arc discharge plasma near the cathode and onto vacuum-chamber walls, J of Surface Investigation. doi:10.1134/S1027451014050401.

[9] Lepeshev AA, Rozhkova EA, Karpov IV, Ushakov AV, Fedorov LYu (2013) Physical, Mechanical, and Tribological Properties of Quasicrystalline Al–Cu–Fe Coatings Prepared by Plasma Spraying, Physics of the Solid State. doi: 10.1134/S1063783413120202.

[10] Ushakov AV, Karpov IV, Lepeshev AA, Petrov MI (2015) Enhancing of magnetic flux pinning in $YBa_2Cu_3O_{7-x}$/CuO granular composites, J Appl Phys. dx.doi.org/10.1063/1.4926549.

[11] Ushakov AV, Karpov IV, Lepeshev AA, Petrov MI Fedorov LYu (2014) Study of Magnetic Flux Pinning in Granular $YBa_2Cu_3O_{7-y}$/nanoZrO_2 Composites, JETP Letters. doi: 10.1134/S002136401402009X.

[12] Ushakov AV, Karpov IV, Lepeshev AA, Petrov MI, Fedorov LYu (2015) Specific Features of the Behavior of Electroarc CuO Nanoparticles in a Magnetic Field, Phys of the Solid State. doi:10.1134/S1063783415050303.

[13] Fukaya K, Sasaki K, Gao J, Kimura T, Watanabe M, Inoue M, Fujimaki A, Sugai H (2009) Analysis of precursors for crystal growth of YBaCuO thin films in magnetron sputtering deposition, Thin Solid Films. doi:10.1016/j.tsf.2008.11.128.

[14] Ushakov AV, Karpov IV, Lepeshev AA (2015) Influence of the Oxygen Concentration on the Formation of Crystalline Phases of ZrO2 Nanoparticles during the Low-Pressure Arc-Discharge Plasma Synthesis, Physics of the Solid State. doi: 10.1134/S1063783415110359.

[15] Pankin NA, Smolanov NA (2011) Molecular-dynamic simulation of ion bombardment with nanoclusters with pair interatomic interaction, Applied Physics 3:39.

[16] Du F, Liu J, Guo Z (2009) Shape controlled synthesis of Cu_2O and its catalytic application to synthesize amorphous carbon nanofibers, J Mater Res Bull. doi:10.1016/j.materresbull.2008.04.011.

[17] Guedes M, Ferreira JMF, Ferro AC (2009) Dispersion of Cu_2O particles in aqueous suspensions containing 4,5-dihydroxy-1,3-benzenedisulfonic acid disodium salt, J Ceram Int. doi:10.1016/j.ceramint.2008.10.023.

[18] Liu J, Huang X, Li Y, Sulieman KM, He X, Sun FJ (2006) Hierarchical nanostructures of cupric oxide on a copper substrate: controllable morphology and wettability, J Mater Chem. doi:10.1039/B611691D.

[19] Keiser JT, Brown CW, Heidersbach RH (1982) The Electrochemical Reduction of Rust Films on Weathering Steel Surfaces, J Electrochem Soc. doi:10.1149/1.2123648.